ANTICANCER RESEARCH
International Journal of Cancer Research and Treatment

Dear Sir/Madam:
Enclosed are the galley proofs of your article for ANTICANCER RESEARCH.

We would like to call your attention to the following:
1. Please read thoroughly, correct, and return the proofs to the Editorial Office within 24 hours.
2. Proofs should be returned by the fastest mail service available. Delays in the return of these proofs will necessitate the publication of your paper in a later issue of the journal. You may also send the proofs by fax or e-mail.
3. Please read the entire manuscript carefully to verify that no changes in meaning have been introduced into the text through language improvements or editorial corrections.
4. Corrections should be limited to typographical errors.
5. To promote rapid publication of articles in ANTICANCER RESEARCH, figures are not sent to the Author(s) unless alterations have been made through the editing process.
6. Should you require reprints, PDF files, issues or subscriptions, please fill the attached reprint order form.
7. Should you require information about your article (publication date, volume, page numbers, etc) please call: +30-22950-52945 or send an e-mail to journals@iiar-anticancer.org.
8. Please provide your complete address (not P.O.B.), telephone and fax numbers.
9. Please feel free to contact us with any queries that you may have (Tel./Fax: +30-22950-53389 or +30-22950-52945, e-mail: journals@iiar-anticancer.org).

Thank you for taking the time to study these guidelines.
Yours,

J.G. Delinassios
Managing Editor

Enclosures

Effect of Ha-*ras*^val12 on *nm23* Expression, Tumor Formation and Metastasis of the Transformants and Immunomodulation in Tumor-bearing Mice

CHANG-CHI HSIEH[1,2], SHAN-YING WU[3], SHENG-HUEI LAN[3],
TZU-YU WENG[3], YU TSAI[4] and HSIAO-SHENG LIU[4,5]

[1]Department of Animal Science and Biotechnology,
Tunghai University, Taichung, Taiwan, ROC;
[2]School of Chinese Medicine Resources, China
Medical University, Taichung, Taiwan, ROC;
[3]Institute of Basic Medical Sciences, College of Medicine,
National Cheng Kung University, Tainan, Taiwan, ROC;
[4]Department of Microbiology and Immunology, College of Medicine,
National Cheng Kung University, Tainan, Taiwan, ROC;
[5]Center for Gene Regulation and Signal Transduction Research,
National Cheng Kung University, Tainan, Taiwan, ROC

Abstract. *Overexpression of the Ha-ras*^val12 *oncogene has frequently been detected in primary and metastatic carcinomas. NM23 is a metastasis inhibition factor and plays a suppressive role in metastasis in many cancers. In this study, a stable NIH/3T3 cell line harboring an inducible Ha-rasval12 oncogene (designated as 7-4) and small interfering RNAs (siRNAs) were used to clarify the reverse correlation between nm23 and Ha-ras expression both in vitro and in vivo. A derivative 7-4/Z-3 cell line harboring a β-galactosidase reporter gene was used to trace cell metastasis in a murine tumor model. The data presented here reveal that Ha-ras*^val12 *is able to cause cell morphological changes, induce tumor formation, and promote metastasis of tumor cells to the lungs. In metastatic mice, the immune surveillance against tumor formation was suppressed by Ha-rasval12 overexpression through an increase in T-reg cells and a decrease of cytotoxic T lymphocytes and natural killer cell populations. Our results suggest that the Ha-ras oncogene regulates morphogenesis, tumorigenesis, and metastasis through suppressing nm23 expression and modulation of immune cell function.*

Correspondence to: Dr. Hsiao-Sheng Liu, Department of Microbiology and Immunology, College of Medicine, National Cheng Kung University, Tainan 70101, Taiwan, ROC. Tel.: +886 62353535 ext. 5630, Fax.: +886 62082705, e-mail: a713@mail.ncku.edu.tw

Overexpression of the Ha-*ras* oncogene has been observed in primary and metastatic human carcinomas. Alterations in Ha-*ras per se* or its expression have also been reported in metastatic tumors (1). Gallick *et al.* examined the expression of the c-ras gene in fresh biopsies from primary and secondary colon carcinomas and found that overexpression of p21^*ras* was common in the primary tumors of Dukes' B and C stages when compared to the surrounding normal tissue (2). In contrast, Sukumar *et al.* demonstrated that about one-third of *N*-methyl-*N*-nitrosourea-induced rat carcinomas expressed the activated c- Ha-*ras* gene (3). The tumor metastatic process is complex, requiring cells to move, invade tissues and basement membranes, avoid immunological responses, and colonize distant sites within the organism (4, 5). However, the mechanism of tumor cell-induced metastasis is poorly understood and the identification of the genes involved is still ongoing. The discovery of such genes may lead to new strategies for diagnostic and therapeutic approaches that help mitigate metastatic events. High *nm23* expression indicated a relatively low metastatic potential in many cell types (1). Although eight human *nm23* homologs have been identified, only H1 and H2 have been extensively studied for their metastasis-related properties. It was shown that aurora-A associates with NM23-H1 and that NM23-H1 further phosphorylates the kinase repressor of Ras, a negative modulator of Ras downstream of the MEK/MAPK pathway (6, 7). The above data suggest that NM23 may be involved in Ha-*ras* -related metastasis process. In addition, overexpression of the NM23-H1 protein may indicate poor survival for

cervical cancer patients (8). However, the relationships of these proteins and their role in metastasis have not yet been determined.

The evasion of immunological surveillance is one of the primary strategies tumor cells utilize in becoming metastatic. Immunological modulation of T lymphocytes by their surface markers may be responsible for the regulation of tumor metastasis (9, 10). The population of regulatory CD4^{+}-T cells expressing the interleukin-2 (IL-2) receptor α-chain (CD25) plays a key role in controlling immunosuppressive capacity both *in vitro* and *in vivo* (11, 12). In this study, we clarified the relationship between Ras and *nm23* and the role of *nm23* in Ras-related tumor formation and metastasis. The effects of the Ha-*ras* oncogene on modulation of immune cells and the ability of Ha-*ras*-transformed cells to suppress immune surveillance and induce metastasis were also investigated.

Materials and Methods

Cell culture. NIH/3T3 and its derivatives, 7-4 and 7-4/Z-3, were maintained in minimum essential medium (MEM) containing 10% calf serum. The 7-4 cells contained the lacI and Ha-*ras* transgenes and the expression of Ha-*ras*[val12] was regulated by the administration of isopropyl β-D-1-thiogalactopyranoside (IPTG) (13). After IPTG induction, the cells were observed at different intervals and the relative expression levels of the Ha-*ras* and *nm23* genes in NIH/3T3 and 7-4 cells were measured by Northern and Western blotting. The 7-4/Z-3 cells harboring the Ha-*ras* oncogene and β-galactosidase reporter gene were detected by histochemical staining using X-gal (14, 15).

Northern blot analysis. Total RNA (20 μg) prepared from the cells was denatured using glyoxal (1.0 M). The denatured RNA was separated in 1% agarose at 80V for 4 h in a 10 mM circulated sodium phosphate (NaPi) buffer system and then transferred to a Hybond-N membrane (Amersham, USA) using 25 mM NaPi buffer. A 4.7 kb Ha-*ras* probe, digested from the pSVlac*Oras* plasmid, was used to detect the expression of the transfected Ha-*ras* construct (13). The *nm23* primers (*nm23-1a*, 5'-CAGTCGCAGCCGGCGGTAAAG-3' and *nm23-1b*, 5'-GCACGTAACACTGCACA-3') were used to amplify a 636 bp fragment by PCR, which was used as a probe to detect the endogenous *nm23* RNA expression. The radioactive probes were hybridized with the RNA-bound membrane and the signals were detected following exposure to Kodak X-OMAT AR film. The quantification of the autoradiograph was done using scanning densitometry (420oe; PDI Inc. USA).

Western blot analysis. Protein expression of Ras in 7-4 cells was induced by different concentrations of IPTG. The cell lysates (50 μg) were separated in a 12% polyacrylamide gel and subsequently transferred to a PVDF membrane (Millipore, USA). After the membranes were blocked with 5% non-fat milk, Ras, NM23, and β-actin proteins were detected using anti-Ras (Oncogene, USA), anti-NM23-H1/H2 (Cell Signaling, UK), and anti-β-actin (Sigma, USA) antibodies, respectively. The reaction was followed by probing with peroxidase-coupled secondary antibodies and then detection using enhanced chemiluminescence (Amersham Pharmacia, USA).

Small interfering RNA (siRNA) transfection. The Ha-*ras*[val12]-specific siRNA was designed and synthesized by Qiagen, Inc (www.qiagen.com). The sense sequence was as follows: 5'-CCGGCAAGAGTGCGCTGACCATCCACTCGAGTGGATGGTC AGCGCAC TCTTGTTTTTG-3'. The cells (5×10^5) were seeded in a 6-cm^2 cell culture dish and incubated in Dulbecco's Modified Eagle medium (DMEM) without antibiotics overnight in a 5% CO_2 incubator. siRNA was transiently transfected into cells using Lipofectamine™ 2000 reagent (Invitrogen Inc, Carlsbad, CA, USA). Briefly, siRNA was diluted in 500 μl of serum-free DMEM to the assigned concentrations (0, 2, 4, 6, and 8 μM). The Lipofectamine-siRNA solution was mixed gently and added to the cells. The cells were incubated at 37°C in a 5% CO_2 incubator for 4 h. The media were then replaced with normal media and the cells were incubated for an additional 48 h before protein extraction.

Inoculation of tumor cells into mice. Male, 6-week-old BALB/c and SCID mice were obtained from the National Laboratory Animal Breeding and Research Center, Taipei, Taiwan. The experimental protocol adhered to the rules of the Animal Protection Act of Taiwan and was approved by the Laboratory Animal Care and Use Committee of the National Cheng Kung University. Mice were randomly divided into the three groups. Using a 28-gauge needle, the mice were injected subcutaneously (*s.c.*) in the back with 0.2 ml of NIH3T3, 7-4 or 7-4/Z-3 cells (2.0×10^6 cells/each side). Briefly, group B was inoculated with NIH3T3 cells, group C was inoculated with 7-4/Z-3 cells and group A was inoculated with PBS alone. Each group contained eight mice and four mice were housed in one cage and provided with sterile food and water ad *libitum*. Tumor sizes were measured with Vernier calipers to calculate the mean diameter at the second and third weeks.

Tumor embedding, sectioning, and X-gal staining. Two weeks post-inoculation with PBS, NIH3T3 and 7-4/Z-3 cells, the lungs and tumors were removed from the injected mice immediately after sacrifice and embedded in cryoresin. The frozen embedded tumors were processed by cryosection using a microtome (Shandon, Pittsburgh, USA). The sections were rinsed with Dulbecco's modified phosphate buffered saline (DPBS) and fixed for 1 h at 4°C with 2% (v/v) formaldehyde and 0.2% (v/v) glutaraldehyde in DPBS. The fixed sections were rinsed with DPBS three times and then stained with staining solution (20 mM potassium ferricyanide, 20 mM potassium ferrocyanide, 2 mM MgCl2, 0.02% [v/v] Nonidet-P40, and 0.01% sodium deoxycholate [w/v] in HEPES buffered DPBS) containing X-gal (1 mg/ml) at 37°C overnight (16).

Lymphocyte preparation from tumor-draining lymph node (TDLN) and splenocytes. Two weeks post-inoculation with PBS, NIH3T3 or 7-4/Z-3 cells, mice were sacrificed by injecting an overdose of sodium pentobarbital. The spleen and superficial inguinal TDLNs of each mouse were collected, weighed, minced finely, and passed through a stainless mesh in RPMI-1640 with 10% fetal bovine serum (FBS). Any residual tissue was further disintegrated by passage through a 21-gauge needle. Erythrocytes in the spleen were lysed for 5 min with 2 ml of lysis solution (0.15 mM NH4Cl, 10 mM KHCO3, and 0.1 mM EDTA, pH 7.2). The cells were washed in Hank's balanced salt solution (HBSS), and the number of viable cells was measured using the trypan blue dye exclusion method.

Table I. *Tumor formation of Ha-rasval12 transformants in mice.*

Group *	Body weight (g)			Tumor diameter (mm)		Tumor weight (g)
	1st wk	2nd wk	3rd wk	2nd wk	3rd wk	
A	27.65±1.50	30.10±1.16	32.99±1.69		-	-
B	27.31±1.50	29.40±1.15	31.90±1.08		-	-
C	27.87±1.44	34.09±2.04	36.89±3.06	4.10±2.22	10.34±3.16	0.55±0.05

*Data presented here as the mean±SD. In each group, eight male mice were used. Group A was inoculated PBS as control, Group B was inoculated NIH3T3 cells that without transformation, Group C was injected with 7-4/Z-3 cells for 2 weeks.

Table II. *Percentage of lymphocyte subtypes in mice after inoculation of PBS, NIH3T3 or 7-4/Z-3.*

Percentage of each subpopulation (%)	Group A (PBS)	Group B (NIH3T3)	Group C (7-4/Z-3)
Spleen			
Weight (g)	0.086±0.007	0.092±0.007	0.149±0.033*
Cell number (×10^7)	5.822±0.443	6.285±0.486	10.795±1.787*
Percentage of each subpopulation (%)			
CD3ε+/CD45+	56.308±2.949	56.580±3.306	60.555±3.203
CD3ε+/CD4+	35.902±3.284	36.917±2.576	45.998±2.704*
CD3ε+/CD8+	19.905±1.634	20.120±1.568	14.212±2.359*
CD3ε+/CD25+	8.248±0.739	8.992±0.460	12.183±2.363*
CD4+/CD25+	6.257±0.512	6.868±0.412	10.145±1.637*
CD19+/CD45+	39.595±3.630	40.877±2.906	39.850±2.565
PanNK+/CD45+	12.322±2.363	12.060±2.356	7.153±1.320*
TDLN			
Cell number (×10^6)	4.007±0.653	4.148±0.483	11.212±3.078*
Percentage of each subpopulation (%)			
CD3ε+/CD45+	88.118±1.788	86.315±1.763	79.755±2.687*
CD3ε+/CD4+	64.980±3.037	63.805±1.810	59.868±4.027
CD3ε+/CD8+	23.125±1.294	21.848±1.267	17.125±1.734*
CD3ε+/CD25+	5.963±0.486	5.992±0.330	7.505±0.353*
CD4+/CD25+	5.337±0.413	5.435±0.288	6.907±0.259*
CD19+/CD45+	11.808±1.449	13.587±1.728	21.897±3.485*
PanNK+/CD45+	4.533±0.476	4.170±0.344	1.618±0.718*

* $P<0.05$, represents a significant difference when compared with Group A which was sham injected with PBS. Data shown as mean±SD. TDLN: Tumor-draining lymph node.

Flow cytometric analysis of splenocytes. The phenotypes of the different lymphocyte populations were determined by the detection of surface markers with specific monoclonal antibodies (mAbs). Briefly, cell suspensions ($5.0×10^5$) were incubated on ice for 30 min in the dark in the presence of fluoresein, phycoerythrin, or PerCP-conjugated mAb (PharMingen, San Diego, USA). Cytofluorometric analysis was performed by laser excitation at 488 nm on the lymphocyte fractions. A computer system (CellQuest; BD Biosciences, Mountain View, CA, USA) was used for data acquisition and analysis. Percentages were calculated on the basis of the number of lymphocytes found in each quadrant. T-cells were identified by expression of the surface marker CD3ε (clone 145-2C11), T-helper cells by CD3ε/CD4 (clone RM4-5), T cytotoxic/suppressor cells by CD3ε/CD8 (clone 53-6.7), B-cells by CD19 (clone 1D3), and natural killer (NK) cells by PanNK (clone DX5). Identification of natural T-reg cells by CD25 (clone PC61) and CD4 markers indicates the cell surface with the interleukin-2 receptor α-chain in T-helper cells (17).

Statistical analysis. The weights of tumor and spleen, and sub-populations of splenocytes are presented as the mean±SD. One-way analysis of variance (ANOVA) was used for statistical analysis. The mean values of two groups were considered significantly different when $P<0.05$.
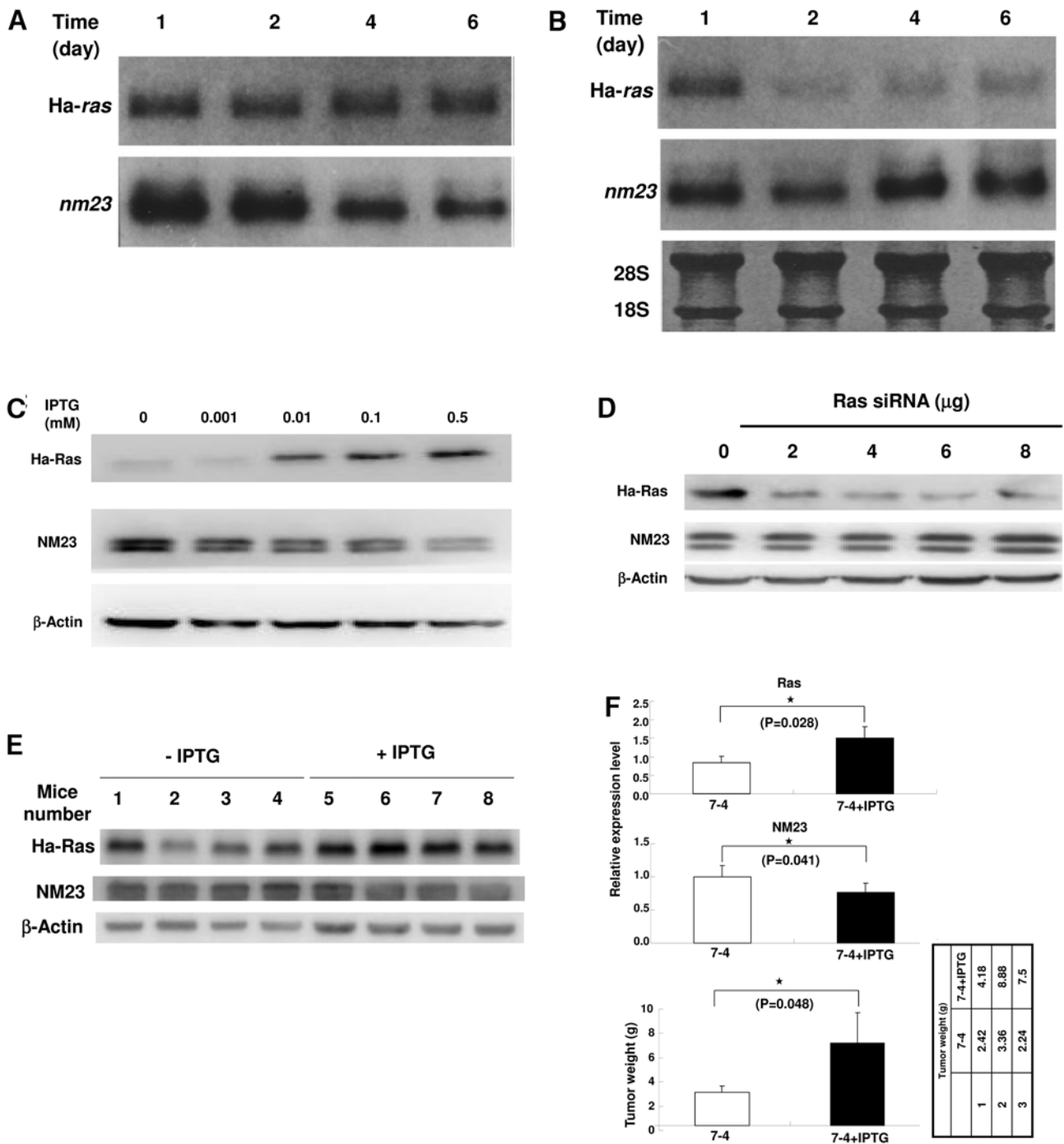
5

Figure 1. *Time course of mRNA and protein expression of Ha-ras val12 and nm23 genes in 7-4 cells. A: The 7-4 cells were induced with IPTG (20 mM) continuously for 6 days. B: The 7-4 cells were induced with IPTG for one day and then grown under normal conditions without IPTG for the remaining days. The total RNA was extracted from treated cells at each time point followed by Northern blotting using the γP32 labeled probes of Ha-ras^{val12} and nm23. 28S and 18S were used as the loading control. C: Total protein was extracted from 7-4 cells in the presence of various dosages of IPTG for 4 days. D: Total protein was extracted from 7-4 cells at treatment with Ras si-RNA at various dosages for 48 h. Antibodies for Ha-ras, NM23 and β-Actin were used to detect each individual gene. E: The 7-4 cells with or without IPTG (5 mM) treatment were injected subcutaneously into SCID mice. Protein was extracted from the tumors to detect Ha-ras and NM23 by Western blotting. β-Actin was used as the internal control. F: Quantification of Ha-ras and NM23 expression levels in Figure 1E as well as the tumor weight in mice with either 7-4 cells with or without IPTG.*
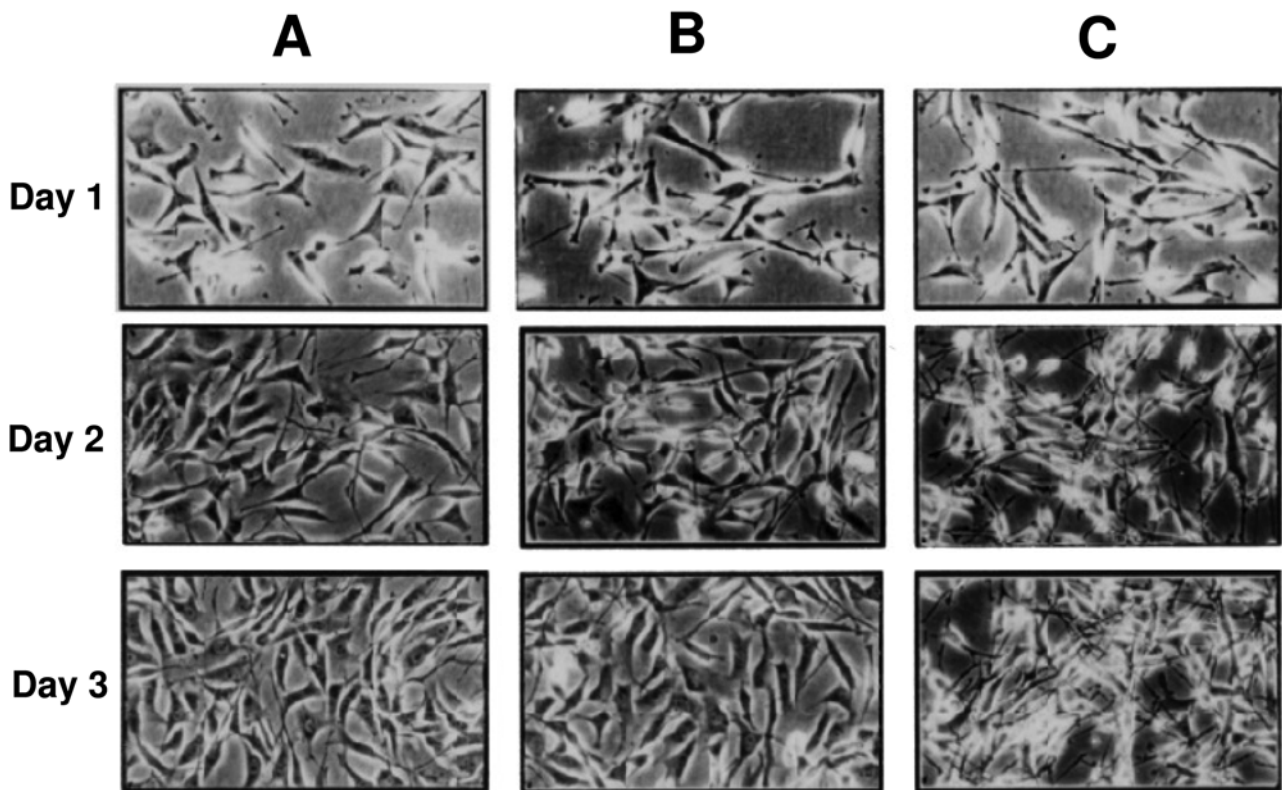
Figure 2. *Morphological changes of 7-4 cells in the presence or absence of IPTG for various times. The morphological change of 7-4 cells with or without IPTG (20 mM) induction for 8 days was investigated. Column A shows the morphology of 7-4 cells without IPTG treatment as a normal control. Column B shows the morphology of 7-4 cells induced with IPTG for one day. IPTG was then withdrawn for the remaining time. Column C shows the morphology of 7-4 cells continuously induced with IPTG for 8 days.*

Results

nm23 gene expression inversely correlates with Ha-ras oncogene expression in Ha-ras transformants. At the transcriptional level, high expression of *nm23* was observed on the first day post-IPTG induction in 7-4 cells. The expression levels of *nm23* in the cells that continuously overexpressed Ha-*ras*val12 gradually declined, felling to half of the amount at day six as compared to the level on the first day post-IPTG induction (Figure 1A). In contrast, the expression levels of *nm23* gradually increased from day one to day six if IPTG was removed one day after induction (Figure 1B). Consistently, IPTG induced Ha-*ras* overexpression at the translational level, in a dose-dependent manner, and NM23 protein expression was inversely suppressed (Figure 1C). Ha-*ras* siRNA suppressed Ras expression in a dose-dependent manner, and the expression of NM23 protein increased conversely (Figure 1D).

The 7-4 cells with or without 24-h IPTG (5 mM) treatment were subsequently injected *s.c.* into SCID mice. Tumor formation was investigated over the subsequent 17

days, and the tumor proteins were then extracted for evaluation of specific protein expression. Our data showed that Ha-*ras* expression was significantly higher in the tumors from the 7-4 cells with IPTG treatment relative to the tumors derived from 7-4 cells without IPTG treatment (Figure 1E and 1F). Consistently, the 7-4 cells with IPTG treatment also induced significantly larger tumor formation compared to 7-4 cells without IPTG treatment (Figure 1F). Conversely, the expression of NM23 was lower in 7-4 cells with IPTG-induced tumors when compared to tumors derived from 7-4 cells without IPTG treatment (Figure 1E and 1F). In summary, our data demonstrate a positive correlation between Ha-*ras* expression and tumor formation and a reverse correlation between Ha-*ras* and NM23 both *in vitro* and *in vivo*.

Ha-ras overexpression causes morphological changes and cell aggregation. The 7-4 cells became round and formed aggregates in the presence of IPTG for 8 days (Figure 2C). In contrast, these same cells without IPTG induction, or incubated in the presence of IPTG for only one day and in
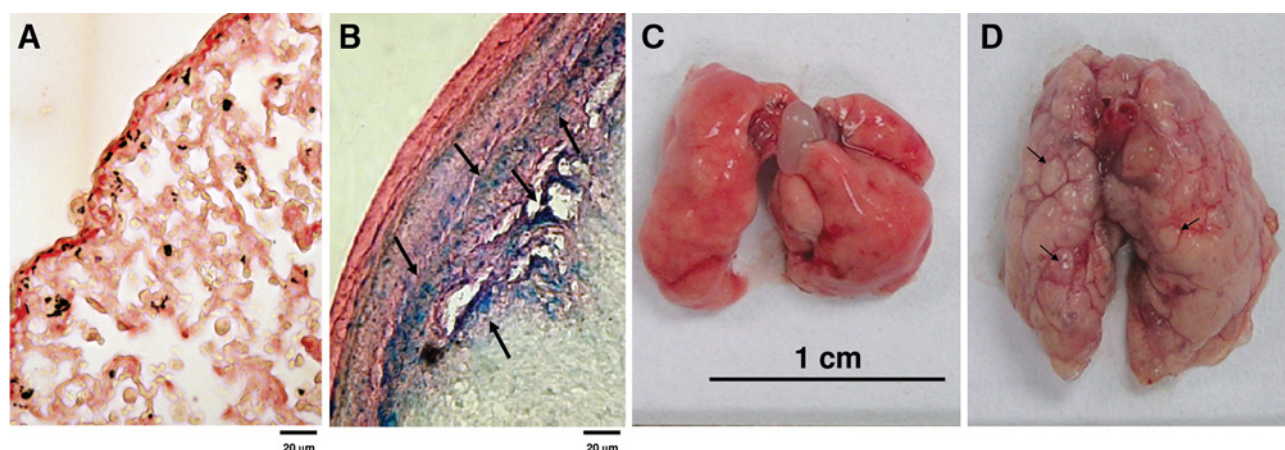
Figure 3. *Tumor formation and metastasis of the Ha-ras transformants in the xenograft mouse model. The 7-4 and 7-4/Z-3 cells were injected intravenously and subcutaneously. into mice, respectively. A: Lung section of the normal mouse. The mice were sacrificed 3 weeks later and cryosections of the lung tissues were stained with X-gal. B: Lung section from a mouse injected with 7-4/Z-3 cells. Arrows indicate the regions with blue staining, representing β-galactosidase expression. C: Lung from the normal mouse sacrificed 3 weeks later. D: Lung from the mouse injected with 7-4 cells for 2 weeks. Arrows point the nodules in the lung.*

the absence of IPTG for the following 7 days, did not become round or form aggregates (Figure 2A and 2B). Our data indicate that Ha-*ras* overexpression changes the cell morphology and causes substantial cell aggregation.

The 7-4 and 7-4/Z-3 cells cause tumor growth and lung metastasis in BALB/c Mice. To determine the potential of the Ha-*ras* transformants for tumor growth and metastasis, 7-4, 7-4/Z-3, control NIH/3T3 cells, or PBS only were injected *s.c.* into BALB/c mice. In the mice injected with 7-4/Z-3 cells, tumors were detected and the size was measured (see Table I). Metastasis of the ras transformants was determined by the detection of positive X-gal stained cells in lung cryosections as well as nodule formation in the lung (Figure 3B and 3D). Our results revealed that 7-4 and 7-4/Z-3 cells harboring Ha-*ras*^{val12} or Ha-*ras*^{val12} and β-galactosidase genes form tumors and also readily migrated from the initial tumor site to the lungs of the inoculated mice.

Ha-ras overexpression affects a sub-population of the immune cells in the spleen and TDLN of the tumor-bearing BALB/c mice. The weight, number of cells, and the lymphocyte sub-populations in the spleen and TDLN of the different groups of mice are shown in Table II. The 7-4/Z-3 tumor-bearing mice (Group C) showed significant increases in spleen weight and the number of splenocytes. The percentage of activated T-reg cells (CD4$^+$/CD25$^+$) of the splenocytes and TDLNs was significantly higher in the 7-4/Z-3 tumor bearing mice when compared to the control group (Group A). In contrast, the percentage of cytotoxic T-cells (CD3ε$^+$/CD8$^+$) and natural killer cells (PanNK$^+$) was

significantly lower in these mice. Together, these data indicate that the Ha-*ras* transformed cell line (7-4/Z-3) modulated the immunity against Ha-*ras* transformants in tumor-bearing mice.

Discussion

Using Rat embryo fibroblast (REF) cells, Steeg demonstrated that adenovirus early region IA (EIA) suppressed the metastatic potential of REFs overexpressing the Ha-*ras* oncogene and the expression of NM23 was also increased (16). This indicates that adenovirus EIA can induce NM23 expression which is involved in the suppression of metastasis. The present study demonstrates that increased tumor formation and lung metastasis correlate with lower *nm23* gene expression. The expression of *nm23* at the transcriptional and translational levels was decreased while Ha-*ras* was continuously overexpressed for 4 days (Figure 1). In this study, the anti-NM23 antibody detects both NM23-H1 and NM23-H2. At least three mechanisms are thought to contribute to the metastasis-suppressive effect of NM23-H1: Firstly, NM23-H1 demonstrates histidine kinase activity toward ATP-citrate lyase, aldolase C, and the kinase suppressor of ras (KSR), with the latter inactivating mitogen-activated protein kinase signaling. Secondly, binding proteins that reduce the availability free NM23-H1 can inhibit its ability to suppress metastasis. Thirdly, NM23-H1 can alter downstream gene expression and demonstrates an inverse association with the lysophosphatidic acid receptor endothelial differentiation gene-28 (EDG2) (18). NM23-H2 is a negative regulator of epidermal growth factor (EGF)- and

Ras-mediated cellular proliferation *via* its effect on the extracellular signal-regulated protein kinase (ERK) pathway (19). The underlying mechanism and signaling pathway(s) that Ha-*ras* influences to suppress NM23 remain to be determined.

The morphology of the transformed cells reverted to the non-transformed form after withdrawal of IPTG (Figure 2, Group B). The *nm23* levels decreased while Ha-*ras* was overexpressed and the cells became round and formed aggregates. These aberrant cell morphologic changes were detected under continuous IPTG induction. We have demonstrated that Ha-*ras*[v12]-induced morphologic change is *via* microtubule disruption and *via* the activation of MEK/ERK signaling pathway that post-translationaly down-regulates Stat3 expression (20). In our murine metastasis model, initially, we demonstrated that all the injected mice formed tumors and in the Ha-*ras* overexpressed tumor, the NM23 level was reduced (Figure 1E and 1F). Furthermore, we revealed that 7-4 and 7-4/Z-3 (harboring a β-galactosidase reporter gene) cells migrated to the lung and form tumors demonstrated by tumor nodules and blue cells labeled by X-gal staining (Figure 3B and 3D). Collectively, we reveal a relationship between Ha-*ras*[val12] overexpression and increased tumor formation, decreased *nm23* expression, cell morphologic changes, as well as the metastasis of the transformants both *in vitro* and *in vivo*.

Immunomodulation of T lymphocytes plays an important role in immune surveillance against tumor cell invasion and metastasis. In this study, we monitored a population of immune cell subtypes in the spleen and TDLNs using immunofluorescence to assess lymphocyte surface antigens. In 7-4/Z-3 tumor-bearing mice, cytotoxic T-cell (CD3ε^{+}/CD8^{+}) and NK (PanNK^{+}/CD45^{+}) populations in the spleen and TDLNs were significantly decreased in 7-4/Z-3 bearing mice. In contrast, CD25^{+}/CD4^{+} T-reg cells in the spleen and TDLNs were significantly increased. This suggests that the increase in T-reg cell numbers might be due to down-regulation of tumor-specific CD8^{+} cytotoxic T lymphocytes (CTLs) and general cytotoxic NK cells, as previously reported. Suppression of CD8+ CTLs and NK cell populations reduces their cytolytic activity and may enhance the initial activation of tumor cells and help sustain tumor growth (21, 22). Clark *et al*. demonstrated the presence of a reduced population of CD8+ CTLs in highly invasive pancreatic cancer (23). Such a microenvironment contributes to the great reduction of tumor-associated myeloid-derived suppressor cells and creates the opportunity for tumor cells to escape from immunosurveillance (24).

In conclusion, *nm23* appears to be responsible for the suppression and regression of tumors, and continuous Ha-*ras* overexpression and tumor formation correlates with down-regulation of *nm23* expression. Our findings shed the light on the regulation between *nm23* and oncogenic Ha-*ras* - associated tumorigenesis as well as metastasis. Ha-*ras* may also increase the metastasis potential of tumor cells through regulation of the activation of T-reg cells and suppressing the immune surveillance of CTLs and NK cells.

References

1　Steeg PS, Bevilacqua G, Kopper L, Thorgeirsson UP, Talmadge JE, Liotta LA and Sobel ME: Evidence for a novel gene associated with low tumor metastatic potential. J Natl Cancer Inst *80*: 200-204, 1988.

2　Gallick GE, Kurzrock R, Kloetzer WS, Arlinghaus RB and Gutterman JU: Expression of p21^{ras} in fresh primary and metastatic human colorectal tumors. Proc Natl Acad Sci USA *82*: 1795-1799, 1985.

3　Sukumar S, Notario V, Martin-Zanca D and Barbacid M: Induction of mammary carcinomas in rats by nitroso-methylurea involves malignant activation of *H-ras-1* locus by single point mutations. Nature *306*: 658-661, 1983.

4　Sugarbaker EV: Patterns of metastasis in human malignancies. Cancer Biol Rev *2*: 235-278, 1981.

5　Fidler IJ and Hart IR: Biological diversity in metastatic neoplasms: Origins and implications. Science *217*: 998-1003, 1982.

6　Du J and Hannon GJ: The centrosomal kinase aurora-A/STK15 interacts with a putative tumor suppressor NM23-H1. Nucleic Acids Res *30*: 5465-5475, 2002.

7　Hartsough MT, Morrison DK, Salerno M, Palmieri D, Ouatas T, Mair M, Patrick J and Steeg PS: *Nm23*-H1 metastasis suppressor phosphorylation of kinase suppressor of ras *via* a histidine protein kinase pathway. J Biol Chem *277*: 32389-32399, 2002.

8　Tee YT, Chen GD, Lin LY, Ko JL and Wang PH: *Nm23*-H1: A metastasis-associated gene. Taiwan J Obstet Gynecol *45*: 107-113, 2006.

9　Wojtowicz-Praga S: Reversal of tumor-induced immunosuppression: A new approach to cancer therapy. J Immunother *20*: 165-177, 1997.

10　Ochsenbein AF, Klenerman P, Karrer U, Ludewig B, Pericin M, Hengartner H and Zinkernagel RM: Immune surveillance against a solid tumor fails because of immunological ignorance. Proc Natl Acad Sci USA *96*: 2233-2238, 1999.

11　Sakaguchi S: Regulatory T-cells: Key controllers of immunologic self-tolerance. Cell *101*: 455-458, 2000.

12　Shevach EM: Certified professionals: CD4(+)CD25(+) suppressor T-cells. J Exp Med *193*: F41-6, 2001.

13　Liu HS, Scrable H, Villaret DB, Lieberman MA and Stambrook PJ: Control of Ha-*ras* -mediated mammalian cell transformation by Escherichia coli regulatory elements. Cancer Res *52*: 983-989, 1992.

14　Liu HS, Chen CY, Lee CH and Chou YI: Selective activation of oncogenic Ha-*ras* -induced apoptosis in NIH/3T3 cells. Br J Cancer *77*: 1777-1786, 1998.

15 Tseng YS, Tzeng CC, Chiu AW, Lin CH, Won SJ, Wu IC and Liu HS: Ha-*ras* overexpression mediated cell apoptosis in the presence of 5-fluorouracil. Exp Cell Res *288*: 403-414, 2003.

16 Steeg PS: Search for metastasis suppressor genes. Invasion Metastasis *9*: 351-359, 1989.

17 Hsieh CC, Lin WC, Lee MR, Hsu SL, Liu HS, Kao ST and Hsieh MT: Dang-gui-bu-xai- tang modulated the immunity of tumor-bearing mice. Immunopharmacol Immunotoxicol *25*: 259-271, 2003.

18 Steeg PS, Horak CE and Miller KD: Clinical-translational approaches to the *nm23*-H1 metastasis suppressor. Clin Cancer Res *14*: 5006-5012, 2008.

19 Lee MY, Jeong WJ, Oh JW and Choi KY: NM23H2 inhibits EGF- and ras-induced proliferation of NIH3T3 cells by blocking the ERK pathway. Cancer Lett *275*: 221-226, 2009.

20 Yeh HH, Wu CH, Giri R, Kato K, Kohno K, Izumi H, Chou CY, Su WC and Liu HS: Oncogenic ras-induced morphologic change is through MEK/ERK signaling pathway to down-regulate Stat3 at a posttranslational level in NIH3T3 cells. Neoplasia *10*: 52-60, 2008.

21 Shimizu J, Yamazaki S and Sakaguchi S: Induction of tumor immunity by removing CD25^{+}CD4^{+} T-cells: A common basis between tumor immunity and autoimmunity. J Immunol *163*: 5211-5218, 1999.

22 Shrikant P and Mescher MF: Control of syngeneic tumor growth by activation of CD8^{+} T-cells: Efficacy is limited by migration away from the site and induction of nonresponsiveness. J Immunol *162*: 2858-2866, 1999.

23 Clark CE, Hingorani SR, Mick R, Combs C, Tuveson DA and Vonderheide RH: Dynamics of the immune reaction to pancreatic cancer from inception to invasion. Cancer Res *67*: 9518-9527, 2007.

24 Clark CE, Beatty GL and Vonderheide RH: Immunosurveillance of pancreatic adenocarcinoma: Insights from genetically engineered mouse models of cancer. Cancer Lett *279*: 1-7, 2009.

April 22, 2010

Dr. Hsiao-Sheng Liu

Re: Your manuscript No. **11107-H**   entitled **«Effect of Ha-*ras*^{val12} on *nm23*...»**

Dear Dr

Referring to your above manuscript for publication in AR, please allow us to use this form letter in reply:

1. *Referee's recommendations:*

   ■ Urgent to be published immediately.

   □ Accepted in the presented form.

   □ Accepted with minor changes.

   ■ Accepted with grammatical or language corrections.

   □ Remarks:

2. *Excess page charges*.

   ■ Your article has approx. **8** printed pages and is in excess of the allotted number by approx. **4** printed pages. The charges are EURO € **210** per excess page, totalling EURO € **840** We ask you to confirm acceptance of these charges.

   ■ Your article includes **1** pages with color figures. The charges are EURO € **650** per color page, totalling EURO € **650**

   TOTAL charges are EURO € 1117.5 (-25% Discount)

   ■ Our invoice will be sent by e-mail to the corresponding author.

3. ■ Your article will appear in Volume **30**, Issue No. **9, 2010**

4. ■ Please order your reprints now. This will facilitate our prompt planning of future issues and rapid publication of your article. Reprints will be delivered by air mail within one month from publication.

We would appreciate your prompt reply.
With many thanks,
Yours sincerely,

J.G. Delinassios
Managing Editor

Please type or print the requested information on the reprint order form and return it to the Editorial Office by fax or e-mail.
Reprints must be paid for in advance.
If your paper is subject to charges for excess pages or color plates, please add these charges to the payment for reprints.
The reprints are not to be sold.

PRICE LIST FOR REPRINTS WITHOUT COVER

Page length	PDF file	Number of copies requested (prices are in Euro)									
		100	200	300	400	500	1000	1500	2000	3000	5000
1-4pp	167	335	387	438	503	554	851	1135	1470	2038	3225
5-8	219	438	503	580	645	722	1083	1445	1832	2554	4012
9-12	277	554	619	709	787	877	1341	1780	2219	3096	4824
13-16	354	709	787	890	993	1096	1625	2141	2657	3676	5715
17-20	419	838	929	1032	1148	1277	1883	2451	3044	4244	6527

For reprints with cover: Please add EURO 140.00 per 100 copies.
Postage: Please add 5% on the above prices.

Reprint Order Form

Of my paper No. **11107-H** comprising **8** printed pages, entitled **«Effect of Ha-*ras*val12 on *nm23...*»**
accepted for publication in ANTICANCER RESEARCH Vol. **30** No. **9**
☐ I require a total of   copies at EURO
☐ I do not require reprints.
☐ Please send me a PDF file of the article at EURO.
☐ Please send me a copy of this issue containing my paper at EURO 45.00.
☐ Please enter my personal subscription to ANTICANCER RESEARCH at the special Author's price of
   EURO 417.00 (print or online); EURO 500.00 (print & online) (☐ Year: 2009).
☐ A check for the above amounts payable to J.G. Delinassios, Executive Publisher of Anticancer Research
   Journal, is enclosed.
☐ Please send an invoice to:

For EC countries: Please give your VAT number:
City and Date: Signature:
Exact postal address:
Tel:
Fax: